

# Interactions of substituted benzenes with elastomers

Shivaputrappa B. Harogopad and Tejraj M. Aminabhavi\*

Department of Chemistry, Karnatak University, Dharwad, 580 003 India

(Received 14 January 1990; revised 1 May 1990, accepted 11 May 1990)

The effects of polymer structure and penetrant molecular size on sorption and diffusion of substituted benzenes (aromatics) with commercial elastomers such as neoprene, ethylene-propylene-diene terpolymer, styrene-butadiene rubber, nitrile-butadiene rubber and natural rubber have been investigated in the temperature interval of 25–60°C. The rate-of-sorption behaviour deviates from the Fickian mechanism. The equilibrium sorption of the sorbents decreases linearly with increasing penetrant molecular size. At about 55–60 mol% uptake, the sorbed concentration levels off. Diffusion coefficients decrease with increasing molecular weight of the penetrants. It is suggested that the hindered chain segmental motion contributes to the overall sorption in addition to strictly thermodynamic considerations. Free-volume concepts can be used to explain the diffusion mechanism through rubbery polymers. Effective values of the molar mass between crosslinks computed from the Flory-Rehner theory appear to vary widely with different liquids and elastomers.

(Keywords: diffusivity; transport; elastomers; penetrants)

## INTRODUCTION

Greater attention is now being devoted to the possible interaction of organic solvents with plastics and elastomers used in a variety of engineering areas<sup>1</sup>. Reduction in a property of a polymeric material in the presence of aggressive solvents may be attributed to chemical degradative processes due to swelling and relaxation of the chain entanglements<sup>2</sup>.

Previous papers from our laboratory reported on the use of a gravimetric method as a rapid and convenient means of studying polymer-solvent interactions, wherein a group of organic solvents were used with a phase-segregated polyurethane<sup>3–5</sup>. The present research extends these studies on the sorption and diffusion behaviour of substituted benzenes (aromatics) with commercial elastomer membranes.

In view of the widespread usage of commercial elastomers such as styrene-butadiene rubber (SBR), nitrile-butadiene rubber (NBR), polychloroprene rubber (CR), ethylene-propylene-diene terpolymer (EPDM) and natural rubber (NR), an effort has been made to investigate their transport characteristics for a number of aromatic solvents. Sorption and diffusion results for benzene, toluene, *p*-xylene, mesitylene and anisole are presented at 25, 44 and 60°C. An effort has been made to evaluate the activation parameters and molar mass between crosslinks of the vulcanized rubbers. Furthermore, the first-order kinetic equation is used to analyse the sorption data.

## EXPERIMENTAL

Moulded sheets of SBR, NBR, CR, EPDM and NR with dimensions of 1/16 inch × 6 inch × 6 inch (~1.6 ×

150 × 150 mm<sup>3</sup>) were obtained from Utex, Weimer, Texas, USA (courtesy of A. Kutac). A 12 inch (~30 cm) laboratory mill was used to mix and prepare the rubber compounds for moulding. The polymer sheets were cured at 160°C for 20 min. Compound formulations along with some representative properties are given in *Table 1*.

Reagent-grade solvents, namely benzene, toluene, *p*-xylene, mesitylene and anisole, were doubly distilled before use. The polymer samples were cut circularly (diameter = 1.94 cm) by means of a sharp-edged steel die. The thickness measurements were made at several points on the membranes using a micrometer screw gauge with an accuracy of ±0.001 cm.

Sorption experiments were performed on cut polymer samples by immersing them in test bottles containing the solvent maintained at the desired temperature in an electric oven (Mettmert, Germany). The experimental details are the same as described earlier<sup>3–5</sup>. The output from a sorption experiment is the per cent fractional weight gain *versus* square root of time ( $t^{1/2}$ ) profile, for different values of the initial thickness ( $h$ ) of the polymer samples.

For a Fickian sorption process, the sorption curves are independent of material thickness. This property of Fickian diffusion can be used to test for the presence of non-Fickian behaviour in the experimental data even when there is a concentration dependence of the mutual diffusion coefficient. If there is a negligible concentration dependence of diffusivity over the concentration interval studied in a sorption experiment, a value of the mutual diffusion coefficient  $D$  can be calculated from the initial slope  $\theta$  of the sorption curve as<sup>6</sup>:

$$D = \pi(h\theta/4Q_\infty)^2 \quad (1)$$

where  $Q_\infty$  represents the maximum equilibrium sorption value for each polymer-solvent pair. It may be noted that the slope  $\theta$  used in equation (1) is calculated from

\* To whom correspondence should be addressed

**Table 1** Elastomer compositions (phr) and their properties

Compounds	SBR	EPDM	CR	NR	NBR
SBR 1500 <sup>a</sup>	100.0	—	—	—	—
EPDM 585 <sup>b</sup>	—	100.0	—	—	—
Neoprene W <sup>c</sup>	—	—	100.0	—	—
NR (RSS-2)	—	—	—	100.0	—
Iycar 1051 <sup>d</sup>	—	—	—	—	100.0
Zinc oxide	5.0	5.0	5.0	5.0	5.0
Carbon black, N550	50.0	50.0	50.0	50.0	50.0
Stearic acid	1.0	1.0	0.5	2.0	1.0
Sulphur	2.0	2.0	—	2.5	2.0
Agerite Resin D <sup>e</sup>	2.0	2.0	—	—	2.0
CBTS <sup>f</sup>	1.0	1.0	—	1.0	1.0
Magnesium oxide	—	—	4.0	—	—
Aranox <sup>g</sup>	—	—	2.0	—	—
END-75 <sup>h</sup>	—	—	0.7	—	—
Bonogen <sup>i</sup>	—	—	—	2.0	—
Agerite Stallite S <sup>j</sup>	—	—	—	2.0	—
Totals	161.0	161.0	162.2	164.5	161.0
Specific gravity	1.15	1.09	1.42	1.14	1.21
Hardness (Shore A)	65	75	78	62	74
Ultimate elongation (%)	420	310	200	600	370
Ultimate tensile (psi)	2840	2050	3320	3510	3320
T <sub>g</sub> (°C)	-42.25	-37.10	-36.21	-57.05	-10.26

<sup>a</sup> Ameripol Synpol<sup>b</sup> Polystar<sup>c</sup> E. I. DuPont de Nemours and Co.<sup>d</sup> B. F. Goodrich<sup>e</sup> Polymerized 1,2-dihydro-2,2,4-trimethylquinoline<sup>f</sup> N-Cyclohexyl-2-benzothiazolesulphenamide<sup>g</sup> N-Phenyl-N'-(p-toluenesulphonyl)-p-phenylenediamine<sup>h</sup> 75% ethylene thiourea (Wyrough and Loser)<sup>i</sup> Sulphonic acid-oil blend<sup>j</sup> Octylated diphenylamine

the sorption curves, which showed linear behaviour before the attainment of 50% of equilibrium.

## RESULTS AND DISCUSSION

Sorption data are interpreted in terms of mole per cent increase in concentration versus square root of time ( $t^{1/2}$ ). Mole per cent of liquid used is defined as moles of liquid absorbed by 100 g of the polymer sample. Some typical plots are given in Figures 1 and 2 at 25°C. For a Fickian diffusion, such plots are linear during the early stages of sorption and reach equilibrium at longer times. If on the other hand, sorption follows the non-Fickian trend, then sorption plots show sigmoidal shapes initially and later level off. Crank and Park offered explanations for such a non-equilibrium phenomenon<sup>7</sup>.

A close inspection of the sorption plots given in Figures 1 and 2 indicates that each polymer behaves differently with different liquids. For instance, in the plots for NR as shown in Figure 1, we find that equilibrium sorption decreases systematically from benzene, toluene, *p*-xylene and mesitylene to anisole. This is also true at higher temperatures, for which plots are not given. Sorption plots of various membranes with benzene at 25°C are displayed in Figure 2. As expected, SBR shows the highest sorption but, during the early stages of sorption, SBR and NR show almost identical sorptivity; at longer times, the total sorption of benzene in NR is smaller than that of SBR. However, NBR, CR and EPDM exhibit more or less identical patterns for the dependence of mole per cent sorption versus  $t^{1/2}$ .

Though the sorption plots of other polymer-solvent systems are not displayed, it would be interesting to

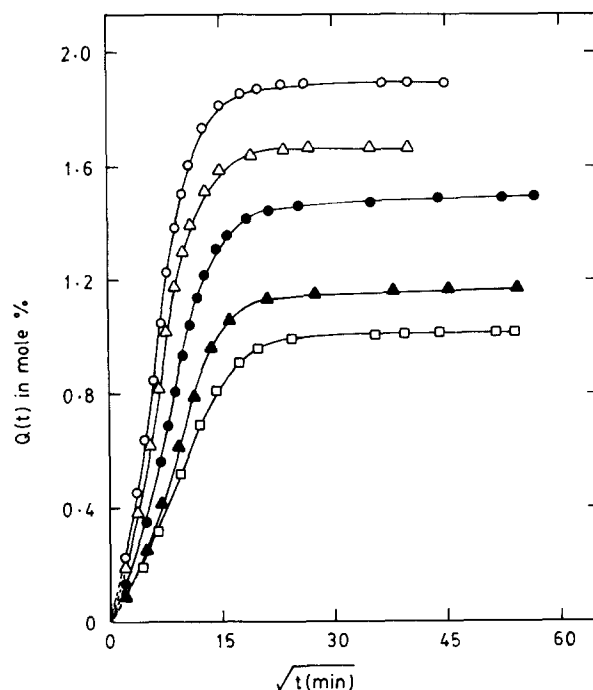


**Figure 1** Mole per cent sorption versus square root of time at 25°C for NR with (○) benzene, (△) toluene, (●) *p*-xylene, (▲) mesitylene and (□) anisole

discuss these data at least on a qualitative basis to show that the sorption tendencies of different polymers with structurally different solvents are not the same. Looking at the maximum sorption data given later in Table 3, it can be inferred that sorption decreases systematically

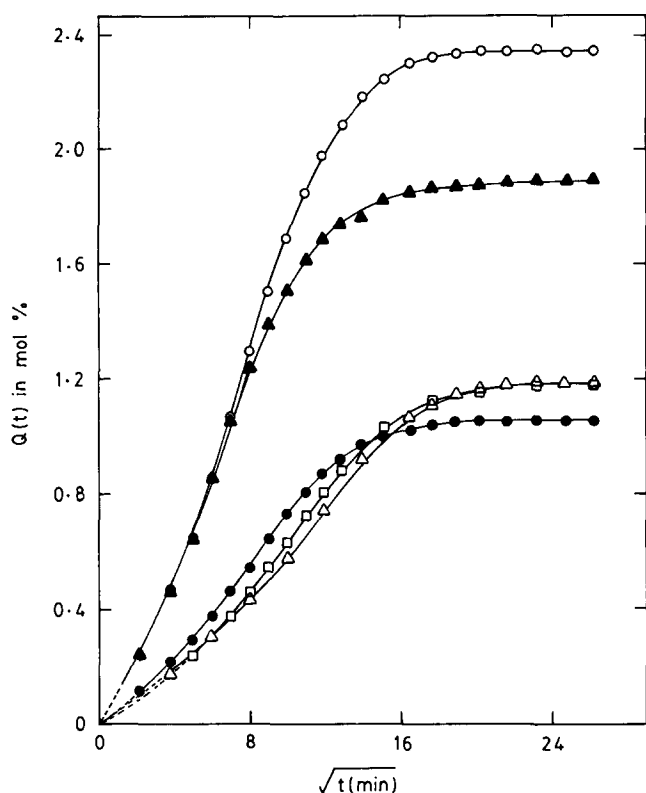


Figure 2 Mole per cent sorption of benzene versus square root of time at 25°C in (○) SBR, (▲) NR, (□) CR, (●) EPDM and (△) NBR membranes

from benzene to mesitylene for all the membranes. However, the sorption tendency of anisole is somewhat different. With NBR, sorption of anisole is even higher than that of benzene; whereas, for SBR, the sorption of anisole is intermediate between that of *p*-xylene and mesitylene. However, with EPDM and NR membranes, anisole absorption is smaller than those of methyl-substituted benzenes.

In the case of neoprene, anisole and *p*-xylene show nearly identical sorption data. In general, of all the membranes, SBR shows high levels of sorption, and this may be attributed to the presence of the aromatic styrene moiety in SBR and to its large surface area, making it susceptible to the aromatic solvents used in this research. The higher sorption values of the NBR–anisole system may be the result of hydrogen-bond type interactions between –CN group of the polymer and –OCH<sub>3</sub> of anisole.

It would also be interesting to offer some comments on the times required to attain equilibrium sorption for the penetrant–polymer systems. For NR, the attainment of sorption equilibrium is much quicker with benzene than with other liquids (cf. Figure 1); and for NBR, the time required to attain equilibrium is quite different for different liquids. For instance, the equilibrium time for anisole is smaller than for benzene and toluene; however, *p*-xylene and mesitylene take longer times to attain equilibrium. With EPDM membrane, the times for attainment of equilibrium remained almost the same for all the methyl-substituted benzenes except anisole. In the case of neoprene, we also observe different sorption equilibrium times, and even the shapes of the sorption curves are quite different.

In order to investigate the type of diffusion mechanism,

the sorption data of all the penetrant–polymer systems have been fitted to the following relation<sup>8</sup>:

$$\log(Q_t/Q_\infty) = \log c + n \log t \quad (2)$$

where  $Q_t$  and  $Q_\infty$  represent the mole per cent increase in concentration at time  $t$  and at equilibrium time  $t_\infty$ . The value of  $n$  decides the type of transport mechanism. A value of  $n = 0.5$  represents the Fickian mechanism and  $n = 1$  indicates the non-Fickian transport. Intermediate values of  $n = 0.5$  to 1.0 suggest the anomalous transport mechanism. The constant  $c$  of equation (2) depends on the structural characteristics of the polymer network in addition to its interaction with the solvent.

From a least-squares analysis, the values of  $n$  and  $c$  have been obtained. It is found that in almost all cases the values of  $n$  vary from 0.5 to 0.7, and thus the transport mechanism is either Fickian or non-Fickian; it may therefore be classified as anomalous. However, we could not observe any systematic dependence of  $n$  on temperature. On the other hand,  $c$  is found to increase steadily with temperature, suggesting an increase in polymer segmental motion with temperature in the presence of the solvent.

According to Southern and Thomas<sup>9,10</sup>, when a polymer film is immersed in a liquid, its surface layer swells immediately but, in the early stages of swelling, the lateral expansion is prevented by the underlying unswollen material. Thus, a two-dimensional compressive stress is developed in the polymer surface. The stress in the surface of the polymer will reduce the equilibrium swelling of the surface layer. As the swelling progresses, the surface area increases; the compressive stress is therefore reduced and the equilibrium swelling of the surface layer increases ultimately to the free unconstrained state. One can therefore use the first-order kinetic equation to study the sorption kinetics:

$$dC/dt = k(C_\infty - C_t) \quad (3)$$

where  $k$  is the first-order rate constant. Integration of equation (3) gives:

$$kt = 2.303 \log[C_\infty/(C_\infty - C_t)] \quad (4)$$

From a least-squares analysis of the plots of  $\log(C_\infty - C_t)$  versus time  $t$ , the values of first-order rate constants  $k$  are calculated. Following the usual conventions in chemical kinetics, we prefer to use  $C_\infty$  and  $C_t$  to express the mole concentrations and these have the same meaning as those of  $Q_\infty$  and  $Q_t$  respectively. The values of activation energies  $E_A$  may be calculated from the temperature dependence of the rate constants. Some typical plots of  $\log(C_\infty - C_t)$  versus  $t$  are shown in Figures 3 and 4.

For all the elastomer–solvent systems the rate constants increase with a rise in temperature. The increase in rate constants for all the methyl-substituted benzenes follows the sequence: NBR < CR < EPDM < SBR < NR. However, this trend is not followed for anisole because CR exhibits lower rate constants than NBR; moreover, the rate constants for anisole are almost identical for both SBR and NR elastomers. Additional support for the use of the first-order sorption kinetics comes from several recently published reports. For instance, Smith and Fisher<sup>11</sup> related solvent uptake to its diffusivity in the polymer structure; the effect of polymer porosity on sorption kinetics has been reported by Poinescu *et al.*<sup>12</sup>. Similarly, Blow<sup>13</sup> has suggested that the mechanism of swelling is essentially a first-order phenomenon.

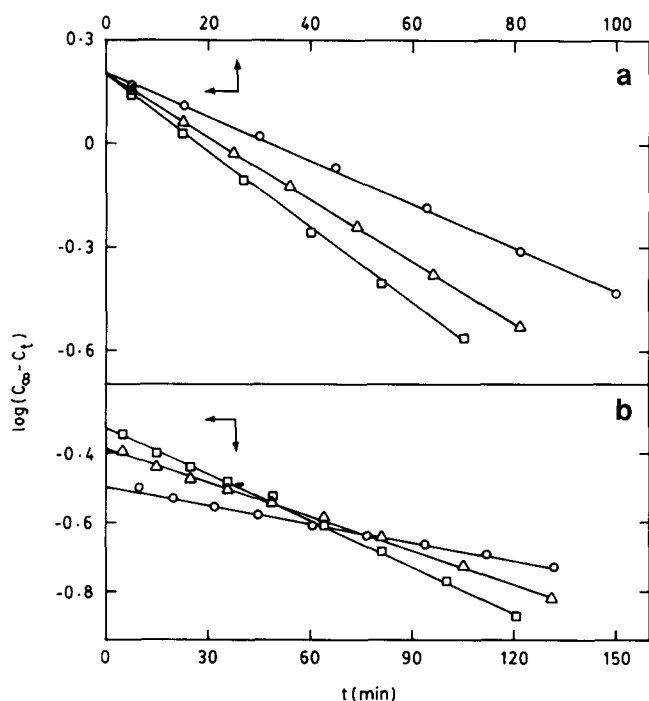


Figure 3 Dependence of  $\log(C_\infty - C_t)$  versus  $t$  for (a) NR-toluene and (b) EPDM-anisole systems at 25°C (O), 44°C (Δ) and 60°C (□)

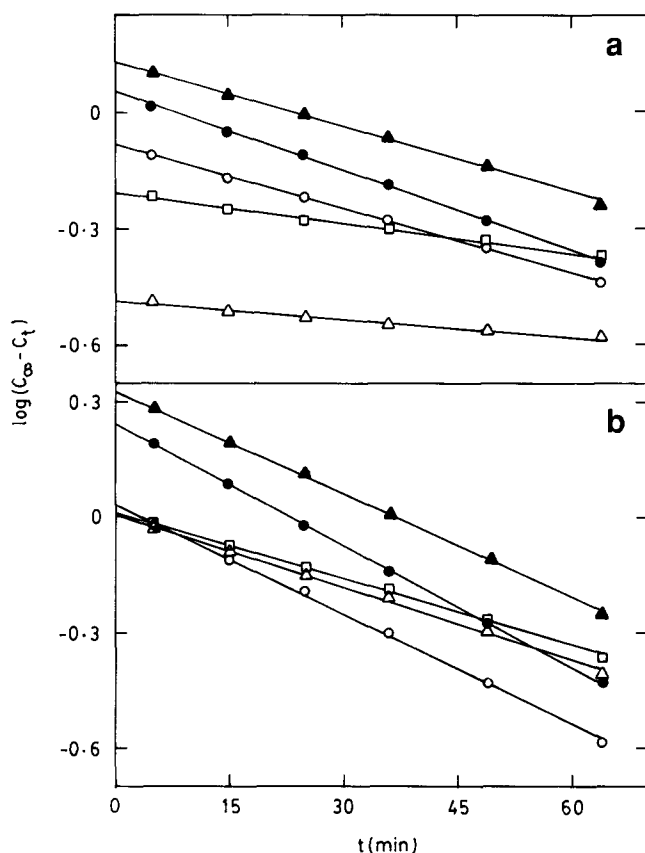


Figure 4 Dependence of  $\log(C_\infty - C_t)$  versus  $t$  for (a) elastomer-mesitylene and (b) elastomer-benzene systems at 60°C: (O) EPDM, (Δ) NBR, (□) CR, (●) NR and (▲) SBR membranes

At any rate, the solvent transport and polymer chain extensions are intimately coupled when the polymer swells from the unperturbed to the solvated state. The increased chain mobility due to swelling allows chain extension, resulting in additional free volume to facilitate

the transport process. The penetrant-induced chain extension is a dynamic relaxation phenomenon and therefore the rate at which the polymer chains reorient affects the rate of solvent transport<sup>1</sup>. A rigorous mathematical analysis of penetrant transport in swelling systems is a formidable problem and therefore we will attempt to analyse the data based on the phenomenological aspects of diffusion processes.

As has already been discussed, the sorption behaviour for most of the penetrants follows a sigmoidal pattern in addition to increase in elastomer dimensions. This led us to consider the diffusion along the three-dimensional axes of circular polymer discs. Following the procedure published by Shen and Springer<sup>14</sup>, the average diffusion coefficients  $\bar{D}$  have been calculated as:

$$\bar{D} = D[1 + (\bar{h}/\bar{r}) + (\bar{h}/2\pi\bar{r})^2] \quad (5)$$

where  $\bar{h}$  and  $\bar{r}$  are the average thickness and average radius of polymer samples. The values of  $D$  used in equation (5) have been calculated from equation (1). The results of  $\bar{D}$  for various elastomer-solvent systems are given in Table 2.

A typical plot for the temperature dependence of  $\bar{D}$  for NBR-solvent systems is shown in Figure 5. In all cases,  $\bar{D}$  is found to be increasing with a rise in temperature. However, with SBR and NR, no systematic variation of  $\bar{D}$  with the size of solvent molecules can be found for the majority of systems. The diffusion coefficients of toluene are higher than for benzene; for mesitylene, diffusivities are smaller than for the remaining methyl-substituted benzenes. This observed anomaly between the penetrant size and diffusivity for methyl-substituted benzenes in the case of SBR and NR might be a true effect and may not be an experimental artifact. On the other hand, with NBR, EPDM and CR we could observe a systematic decrease in  $\bar{D}$  values with an increase in the size of the penetrant molecule, except that of EPDM-toluene system at 60°C. The diffusion trend of anisole is in between toluene and *p*-xylene for all the elastomers except NR; for the latter, it is in between *p*-xylene and mesitylene.

It is interesting to look into the values of  $\bar{D}$  for various elastomer-penetrant systems. For instance, diffusivities are higher for NR than for the remaining elastomers for all the solvents. The diffusivity trends of all the solvents

Table 2 Diffusion coefficients  $\bar{D} \times 10^7$  (cm<sup>2</sup> s<sup>-1</sup>) for elastomer-solvent systems

Solvent	Temp. (°C)	SBR	NBR	EPDM	CR	NR
Benzene	25	12.5	4.9	11.6	8.4	13.7
	44	19.1	9.0	18.6	13.2	21.5
	60	26.5	13.8	26.0	19.2	30.4
Toluene	25	16.3	4.1	10.4	8.2	13.7
	44	21.8	6.9	18.6	12.4	22.2
	60	26.3	10.1	28.0	16.3	32.2
<i>p</i> -Xylene	25	5.6	1.3	6.0	3.6	6.8
	44	9.8	3.0	10.3	6.5	12.5
	60	14.8	5.9	14.6	9.6	19.0
Mesitylene	25	5.1	0.6	4.6	2.9	6.5
	44	9.1	1.3	7.9	4.9	11.4
	60	14.4	2.5	13.2	7.4	16.0
Anisole	25	6.9	3.3	4.5	5.0	7.0
	44	9.0	5.6	7.6	7.1	9.3
	60	11.1	8.2	10.8	9.8	11.5

tend to follow the sequence: NR > SBR > EPDM > CR > NBR. This sequence is true at all temperatures (see Table 2). However, the maximum mole per cent sorption,  $Q_\infty$ , also represents the true equilibrium sorption constant,  $K_s$  (expressed as moles of solvent per 100 g of the polymer), for each polymer-solvent system. These values as summarized in Table 3 suggest the general sequence: SBR > NR > CR > EPDM > NBR. This sequence is true for methyl-substituted benzenes. In any case, there appears to be no correlation between the sequential trend of sorption and diffusion phenomena.

The diffusion process in rubbery polymers has been explained in terms of free-volume theory<sup>15,16</sup>. According to this theory, the rate of diffusion of a molecule depends primarily on the ease with which polymer chain segments exchange their positions with penetrant molecules. The mobility of the polymer in turn depends on the amount of free volume in the matrix. The ease of exchange

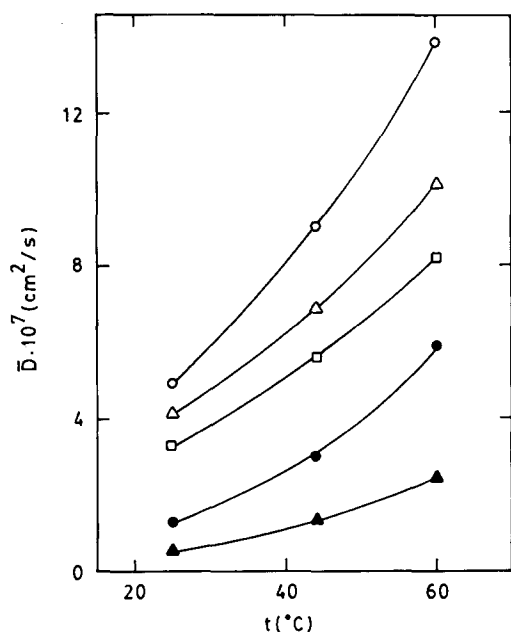


Figure 5 Diffusion coefficients versus temperature for NBR. Symbols have the same meaning as in Figure 1

becomes less as the penetrant size increases, leading to a decrease in the diffusion coefficient.

Conventionally, it is also possible to calculate the activation energy for diffusion,  $E_D$ , by considering the solvent transport to be an activated process by using:

$$\log \bar{D} = \log D_0 - E_D/2.303RT \quad (6)$$

Typical Arrhenius plots of  $\log \bar{D}$  versus  $1/T$  for NBR and SBR elastomers are given in Figure 6. The estimated values of  $E_D$  are compiled in Table 4 along with the activation energy  $E_A$  as estimated from the temperature

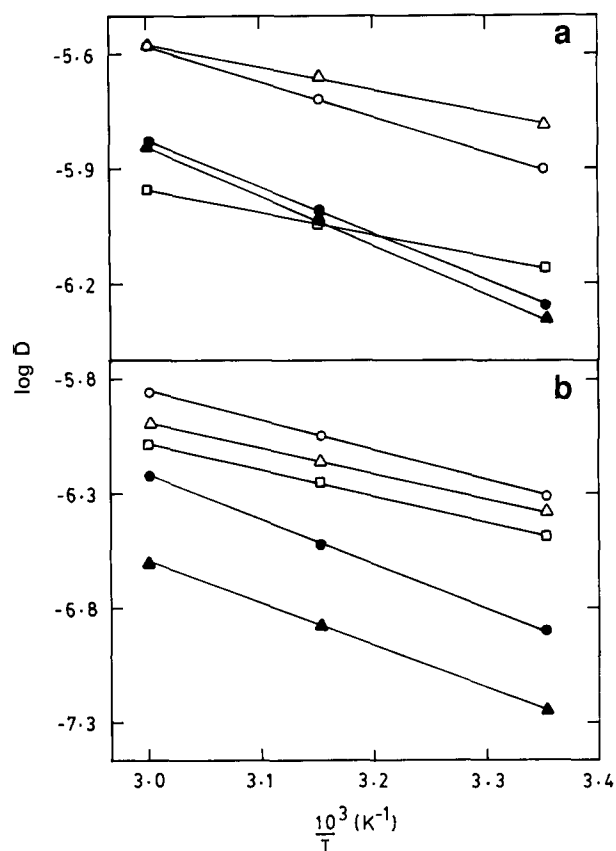


Figure 6 Arrhenius plots ( $\log \bar{D}$  vs.  $1/T$ ) for (a) SBR and (b) NBR. Symbols have the same meaning as in Figure 1

Table 3 Temperature dependence of sorption constants  $K_s$  (mol%) for elastomer-solvent systems

Elastomer	Temp. (°C)	Benzene	Toluene	p-Xylene	Mesitylene	Anisole
SBR	25	2.345	2.021	1.757	1.484	1.602
	44	2.270	1.970	1.739	1.436	1.619
	60	2.242	1.900	1.710	1.420	1.630
NBR	25	1.183	0.824	0.661	0.354	1.378
	44	1.135	0.794	0.635	0.336	1.321
	60	1.096	0.758	0.611	0.345	1.283
CR	25	1.182	1.004	0.916	0.700	0.890
	44	1.161	0.989	0.886	0.680	0.922
	60	1.098	0.922	0.871	0.666	0.881
EPDM	25	1.051	1.085	1.048	0.908	0.361
	44	1.110	1.092	1.043	0.887	0.451
	60	1.161	1.093	1.040	0.879	0.519
NR	25	1.894	1.669	1.498	1.170	1.017
	44	1.879	1.654	1.481	1.186	1.109
	60	1.875	1.671	1.450	1.189	1.211

**Table 4** Activation parameters  $E_D$  and  $E_A$  ( $\text{kJ mol}^{-1}$ ), van't Hoff parameters  $\Delta H_s$  ( $\text{kJ mol}^{-1}$ ) and  $\Delta S$  ( $\text{J mol}^{-1} \text{ } ^\circ\text{C}^{-1}$ ) and molar mass  $M_c$  between crosslinks for elastomer-solvent systems

Penetrant	Property	SBR	NBR	CR	EPDM	NR
Benzene	$E_A$	12.09	20.30	16.24	17.49	10.50
	$E_D$	17.78	24.47	19.51	19.06	18.88
	$\Delta H_s$	-1.08	-1.80	-1.71	2.34	-0.24
	$\Delta S$	-34.83	-42.90	-42.54	-30.02	-33.81
	$M_c$	947	260	347	1337	1069
Toluene	$E_A$	9.81	20.24	14.37	14.91	12.80
	$E_D$	11.39	21.15	16.21	23.37	20.18
	$\Delta H_s$	-1.44	-1.94	-1.95	0.18	0.01
	$\Delta S$	-37.24	-46.38	-44.72	-37.01	-34.04
	$M_c$	830	182	344	718	1477
<i>p</i> -Xylene	$E_A$	16.59	25.68	19.69	20.00	14.21
	$E_D$	23.16	36.34	23.39	21.26	24.42
	$\Delta H_s$	-0.63	-1.84	-1.27	-1.80	-0.75
	$\Delta S$	-35.69	-47.89	-43.10	-38.51	-37.42
	$M_c$	1637	236	752	827	1175
Mesitylene	$E_A$	16.22	23.25	20.75	20.17	15.84
	$E_D$	24.73	35.25	21.91	25.04	21.21
	$\Delta H_s$	1.031	-0.72	-1.19	-0.78	0.387
	$\Delta S$	-38.49	-49.44	-45.26	-41.72	-35.68
	$M_c$	1081	270	686	664	1824
Anisole	$E_A$	16.28	22.28	18.33	21.50	13.23
	$E_D$	11.08	21.54	15.65	20.69	11.65
	$\Delta H_s$	0.40	-1.68	-0.17	8.66	4.09
	$\Delta S$	-33.04	-41.28	-39.72	-17.70	-24.47
	$M_c$	1634	438	892	<i>a</i>	2692

<sup>a</sup> Negative value obtained

dependence of rate constants. In most cases, the values of  $E_D$  are higher than  $E_A$ . Activation energies, except that of toluene, seem to be increasing from benzene to mesitylene in the case of CR and EPDM; however, with NR,  $E_A$  increases all the way from benzene to mesitylene. Differences in the values of  $E_A$  are attributed to differences in polymer structures in addition to the nature of interacting groups of the solvent molecules. The values of  $K_s$  are seen to be related to the penetrant molecular size. Figure 7 shows the linear dependence of  $K_s$  on molecular weight of the penetrants. The decrease in sorption constant as a function of molecular size of the penetrant can be attributed to the fact that benzene, being small in size, may be sorbed in a larger amount than its methyl-substituted analogues. Thus, it appears that sorption is governed not only by the differences in solubility parameters of the solvents but also by differences in the polymer molecular structure, in addition to the size of the penetrant molecule. Furthermore, with all the penetrants, sorption might effectively take place only in the pre-existing volume of the elastomer. The hole size decreases exponentially and therefore the available volume for sorption decreases when the penetrant molecular size increases. As a further consequence of sorption in the elastomer matrix, one might anticipate that the molecular structure of the polymer and the shape of the penetrant molecule also would play a role in the determination of  $K_s$ . This is confirmed by the data shown in Figure 7 for EPDM (a hydrophobic polymer), where there is no pronounced decrease in  $K_s$  values from benzene to mesitylene.

From the results of sorption constants  $K_s$  given in Table 3, efforts have been made to estimate the enthalpy  $\Delta H_s$  and entropy  $\Delta S$  of sorption by making use of the van't Hoff relation:

$$\log K_s = (\Delta S/2.303R) - (\Delta H_s/2.303R)(1/T) \quad (7)$$

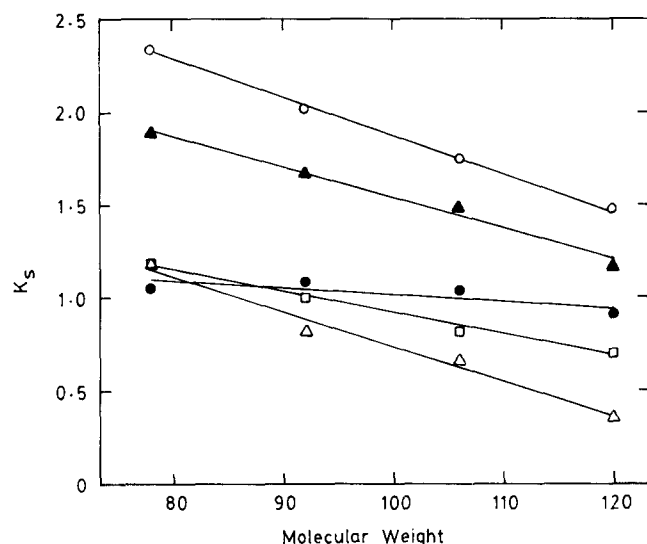


**Figure 7** Equilibrium sorption constant versus molecular weight of solvents for (○) SBR, (▲) NR, (□) CR, (●) EPDM and (△) NBR membranes

A typical van't Hoff plot for NBR with all the solvents is shown in Figure 8 and the estimated values of  $\Delta H_s$  and  $\Delta S$  at the 95% confidence level are also included in Table 4. It is noticed that, for the majority of elastomer-solvent systems,  $\Delta H_s$  is negative, suggesting the sorption to be an exothermic process. However, for all the elastomer-solvent systems,  $\Delta S$  values are negative, suggesting the orderliness of the liquid structure in the sorbed state within the polymer matrix.

In order to gain further insight into the sorption process in relation to the morphological characteristics of the

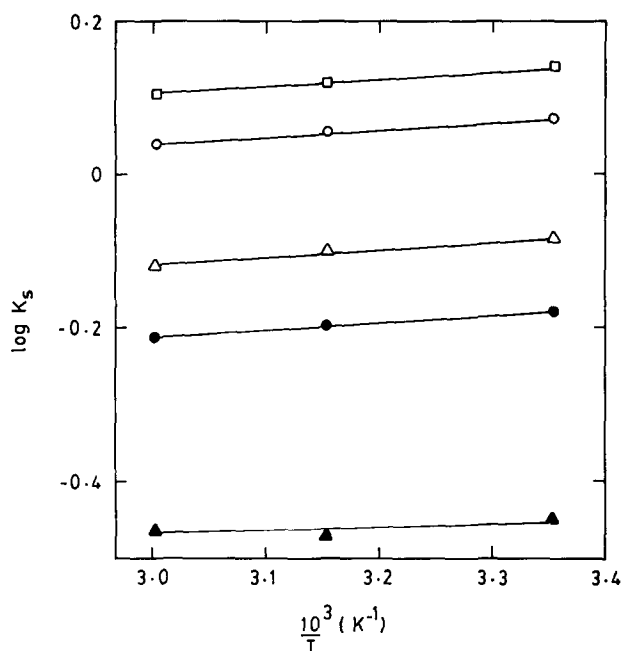


Figure 8 van't Hoff plots ( $\log K_s$  vs.  $1/T$ ) for NBR. Symbols have the same meaning as in Figure 1

elastomers, efforts have been directed towards an understanding of the relation between molar mass  $M_c$  between crosslinks and diffusivity. Whenever a polymer is immersed in an organic liquid, its molecules will diffuse into the solid polymer film to produce a swollen gel. Dissolution is prevented if the attraction between neighbouring polymer molecules is sufficiently great, perhaps due to crosslinking. Swelling equilibrium is approached when the chemical potential of the solvent inside the swollen polymer becomes equal to that of the outside phase. This phenomenon can be studied in terms of the Flory–Rehner model<sup>17,18</sup>:

$$v_e/V = -[\ln(1 - \phi) + \phi + \chi\phi^2]/V_s(\phi^{1/3} - \phi/2) \quad (8)$$

where  $v_e/V$  represents the concentration of the elastically effective network chains,  $V_s$  is molar volume of solvent,  $V$  is volume of the unswollen polymer and  $\phi$  is volume fraction of polymer in the fully swollen state. If the interaction parameter  $\chi$  is known for the elastomer–solvent pair, then the molar mass  $M_c$  between network crosslinks can be calculated as:

$$M_c = -\rho V_s(\phi^{1/3} - \phi/2)/[\ln(1 - \phi) + \phi + \chi\phi^2] \quad (9)$$

where  $\rho$  is the density of the polymer. The parameter  $\chi$  can be obtained from a modification of the Flory–Rehner theory as:

$$\chi = \frac{[N + (N/\phi)\ln(1 - \phi) + 1/(1 - \phi)]}{[2 - \phi N - (\phi/T)(\partial\phi/\partial T)]} \quad (10)$$

where

$$N = \left(\frac{\phi^{2/3}}{3} - \frac{2}{3}\right)/(\phi^{1/3} - 2\phi/3).$$

The calculated values of  $M_c$  are also included in Table 4.

The  $M_c$  values are generally higher for SBR and EPDM than for NBR; with the latter,  $M_c$  ranges from 180 to 440. In all cases,  $M_c$  data seem to depend on the solvent and there appears to be no correlation between the size of the penetrant and the  $M_c$  data. In any case, the results can be explained in relation to the diffusion data. The

decrease in chain mobility caused by increased crosslinking as manifested by lower values of  $M_c$  has been found to increase the activation energy for diffusion, thereby showing lower values of diffusion coefficients<sup>19</sup>. Both the increase in activation energy and the proportionate decrease in the diffusion coefficient become greater as the size of the diffusing molecule increases, suggesting that at high crosslink densities there is a tendency for the diffusion medium to act as a molecular sieve in the same manner as with inorganic zeolites<sup>20</sup>. Since all the elastomer samples contained a high loading of reinforcing filler, this might have affected the changes in  $M_c$  values from one solvent to another.

## CONCLUSIONS

In the present study, five monocyclic aromatics have been investigated as to their interaction with five different elastomers of commercial interest. Several parameters such as kinetic rate constants, sorption constants, diffusion coefficients, activation energies, enthalpy and entropy of activation in addition to molar mass between crosslinks have been studied. A knowledge of these properties was helpful in arriving at quantitative conclusions as to the mechanism of interactions. The gravimetric method used here was of practical value in obtaining both kinetic and thermodynamic data from sorption experiments, especially when there is a need to evaluate or screen a number of liquids as to their potential interaction with a polymeric material. Research in this field is continuing and these results will be reported in subsequent publications.

## ACKNOWLEDGEMENTS

We thank the University Grants Commission, Delhi, for the award of a FIP fellowship to SBH to study for a PhD at Karnatak University and to Professor P. E. Cassidy of Southwest Texas State University for a supply of polymer samples.

## REFERENCES

- 1 Aminabhavi, T. M., Aithal, U. S. and Shukla, S. S. *J. Macromol. Sci., Rev. Macromol. Chem. Phys. (C)* 1988, **28** (3 & 4), 421
- 2 Aminabhavi, T. M., Aithal, U. S. and Shukla, S. S. *J. Macromol. Sci., Rev. Macromol. Chem. Phys. (C)* 1989, **29** (2 & 3), 319
- 3 Aithal, U. S., Aminabhavi, T. M. and Cassidy, P. E. *Polym. Prepr.* 1989, **30** (1), 17
- 4 Aithal, U. S. and Aminabhavi, T. M. *J. Chem. Educ.* 1990, **67**, 82
- 5 Aithal, U. S. and Aminabhavi, T. M. *Polymer* 1990, **31**, 1757
- 6 Crank, J. 'The Mathematics of Diffusion', 2nd Edn., Clarendon, Oxford, 1975
- 7 Crank, J. and Park, G. S. *Trans. Faraday Soc.* 1949, **45**, 240
- 8 Lucht, L. M. and Peppas, N. A. *J. Appl. Polym. Sci.* 1987, **33**, 1557
- 9 Southern, E. and Thomas, A. G. *J. Polym. Sci. (A)* 1965, **3**, 641
- 10 Southern, E. and Thomas, A. G. *Trans. Faraday Soc.* 1967, **63**, 1913
- 11 Smith, P. M. and Fisher, M. M. *Polymer* 1984, **25**, 84
- 12 Poinescu, Ig. C., Beldi, C. and Vlad, C. *J. Appl. Polym. Sci.* 1984, **29**, 23
- 13 Blow, C. M. (Ed.) 'Rubber Technology and Manufacture'. 2nd Edn., Butterworth Scientific, London, 1982, pp. 73–4
- 14 Shen, C. H. and Springer, G. S. *J. Polym. Compos.* 1976, **10**, 2
- 15 Fujita, H. *Adv. Polym. Sci.* 1961, **3**, 1
- 16 Fujita, H. and Kishimoto, A. *J. Polym. Sci.* 1958, **25**, 547
- 17 Flory, P. J. and Rehner, J. *J. Chem. Phys.* 1943, **11**, 521
- 18 Flory, P. J. 'Principles of Polymer Chemistry', Cornell University, Ithaca, NY, 1953
- 19 Park, G. S. in 'Treatise in Coatings' (Ed. R. R. Myers), Dekker, New York, 1976, p. 473
- 20 Barrer, R. M. and Ibbitson, D. A. *Trans. Faraday Soc.* 1944, **40**, 195